

Modulation of the second-harmonic generation in MoS_2 by graphene covering

Chunchun Wu(吴春春), Nianze Shang(尚念泽), Zixun Zhao(赵子荀), Zhihong Zhang(张智宏), Jing Liang(梁晶), Chang Liu(刘畅), Yonggang Zuo(左勇刚), Mingchao Ding(丁铭超), Jinhuan Wang(王金焕), Hao Hong(洪浩), Jie Xiong(熊杰), and Kaihui Liu(刘开辉)\cccclink

Citation: Chin. Phys. B, 2021, 30 (**2**): 027803. DOI: 10.1088/1674-1056/abd77f
Journal homepage: http://cpb.iphy.ac.cn; http://iopscience.iop.org/cpb

What follows is a list of articles you may be interested in

Quantum plasmons in the hybrid nanostructures of double vacancy defected graphene and metallic nanoarrays

Rui Tang(唐睿), Yang Xu(徐阳), Hong Zhang(张红), and Xin-Lu Cheng(程新路)
Chin. Phys. B, 2021, 30 (**1**): 017804. DOI: 10.1088/1674-1056/abaedb

Visible-to-near-infrared photodetector based on graphene-$MoTe_2$-graphene heterostructure

Rui-Xue Hu(户瑞雪), Xin-Li Ma(马新莉), Chun-Ha An(安春华), Jing Liu(刘晶)
Chin. Phys. B, 2019, 28 (**11**): 117802. DOI: 10.1088/1674-1056/ab4576

Efficient doping modulation of monolayer WS_2 for optoelectronic applications

Xinli Ma(马新莉), Rongjie Zhang(张荣杰), Chunhua An(安春华), Sen Wu(吴森), Xiaodong Hu(胡晓东), Jing Liu(刘晶)
Chin. Phys. B, 2019, 28 (**3**): 037803. DOI: 10.1088/1674-1056/28/3/037803

Raman spectroscopy characterization of two-dimensional materials

Fang Liang(梁芳), Hejun Xu(徐何军), Xing Wu(吴幸), Chaolun Wang(王超伦), Chen Luo(骆晨), Jian Zhang(张健)
Chin. Phys. B, 2018, 27 (**3**): 037802. DOI: 10.1088/1674-1056/27/3/037802

Different angle-resolved polarization configurations of Raman spectroscopy: A case on the basal and edge plane of two-dimensional materials

Xue-Lu Liu(刘雪璐), Xin Zhang(张昕), Miao-Ling Lin(林妙玲), Ping-Heng Tan(谭平恒)
Chin. Phys. B, 2017, 26 (**6**): 067802. DOI: 10.1088/1674-1056/26/6/067802

RAPID COMMUNICATION

Modulation of the second-harmonic generation in MoS_2 by graphene covering*

Chunchun Wu(吴春春)[1,2,†], Nianze Shang(尚念泽)[2,†], Zixun Zhao(赵子荀)[2,†], Zhihong Zhang(张智宏)[2], Jing Liang(梁晶)[2], Chang Liu(刘畅)[2], Yonggang Zuo(左勇刚)[3], Mingchao Ding(丁铭超)[3], Jinhuan Wang(王金焕)[2], Hao Hong(洪浩)[2,‡], Jie Xiong(熊杰)[1,§], and Kaihui Liu(刘开辉)[2,¶]

[1] *State Key Laboratory of Electronic Thin Films and Integrated Devices, University of Electronic Science and Technology of China, Chengdu* 610054, *China*
[2] *State Key Laboratory for Mesoscopic Physics and Frontiers Science Center for Nano-optoelectronics, Collaborative Innovation Center of Quantum Matter, Academy of Advanced Interdisciplinary Studies, School of Physics, Peking University, Beijing* 100871, *China*
[3] *Institute of Physics, Chinese Academy of Sciences, Beijing* 100080, *China*

(Received 8 December 2020; revised manuscript received 18 December 2020; accepted manuscript online 30 December 2020)

Nonlinear optical frequency mixing, which describes new frequencies generation by exciting nonlinear materials with intense light field, has drawn vast interests in the field of photonic devices, material characterization, and optical imaging. Investigating and manipulating the nonlinear optical response of target materials lead us to reveal hidden physics and develop applications in optical devices. Here, we report the realization of facile manipulation of nonlinear optical responses in the example system of MoS_2 monolayer by van der Waals interfacial engineering. We found that, the interfacing of monolayer graphene will weaken the exciton oscillator strength in MoS_2 monolayer and correspondingly suppress the second harmonic generation (SHG) intensity to 30% under band-gap resonance excitation. While with off-resonance excitation, the SHG intensity would enhance up to 130%, which is conjectured to be induced by the interlayer excitation between MoS_2 and graphene. Our investigation provides an effective method for controlling nonlinear optical properties of two-dimensional materials and therefore facilitates their future applications in optoelectronic and photonic devices.

Keywords: two-dimensional materials, second harmonic generation (SHG), graphene, dielectric screening

PACS: 78.67.Wj, 42.65.−k **DOI:** 10.1088/1674-1056/abd77f

1. Introduction

Group VI transition-metal dichalcogenides (TMDs), the representative two-dimensional (2D) materials, have brought us plentiful physics, including strongly bound excitons, valley-selective circular dichroism, 2D topological insulating states, etc.[1–11] Among these exciting physical properties, efficient nonlinear optical responses, ranging from second harmonic generation (SHG) to high harmonic generation (HHG) have been found in these atomically thin layered materials and attracted tremendous scientific interests.[12–17] These strong nonlinear optical responses are the fundamental building blocks in the design of advanced optics devices and also bring us unique techniques in material characterization.[18–21] Manipulation and engineering of the nonlinear properties of 2D materials are of paramount importance for realizing practical devices. Previously, some methods have been proposed to achieve the modulation of nonlinear optical response in 2D materials, including coupling with waveguides, suffering electron doping or in-plane strain, etc.[22–30] However, those methods are either complicated in fabrication processes or limited by specific substrates. Therefore, new mechanisms for facile and efficient nonlinear optical response manipulation are still on the way for further exploration.

Van der Waals interfacial engineering is supposed to be an efficient approach to modulate the physical properties of 2D materials. Benefiting from the atomically thin structure, the electron wave functions of 2D materials are distributed at the surface, leading to their sensitive responses to interfacial interaction such as the van der Waals forces.[31] Recent works have revealed their tunability in electronic, mechanical, optical properties by van der Waals stacking.[32,33] For examples, flat

*Project supported by Beijing Natural Science Foundation, China (Grant No. JQ19004), Beijing Excellent Talents Training Support, China (Grant No. 2017000026833ZK11), the National Natural Science Foundation of China (Grant Nos. 52025023, 51991340, and 51991342), the National Key Research and Development Program of China (Grant Nos. 2016YFA0300903 and 2016YFA0300804), the Key R&D Program of Guangdong Province, China (Grant Nos. 2019B010931001, 2020B010189001, 2018B010109009, and 2018B030327001), the Beijing Municipal Science & Technology Commission, China (Grant No. Z191100007219005), the Beijing Graphene Innovation Program (Grant No. Z181100004818003), Bureau of Industry and Information Technology of Shenzhen (Graphene platform 201901161512), Guangdong Innovative and Entrepreneurial Research Team Program (Grant No. 2016ZT06D348), the Science, Technology and Innovation Commission of Shenzhen Municipality (Grant No. KYTDPT20181011104202253), and the China Postdoctoral Science Foundation (Grant No. 2020M680177).

†These authors contributed equally to this work.
‡Corresponding author. E-mail: haohong@pku.edu.cn
§Corresponding author. E-mail: jiexiong@uestc.edu.cn
¶Corresponding author. E-mail: khliu@pku.edu.cn

© 2021 Chinese Physical Society and IOP Publishing Ltd

band and superconductivity were observed in bilayer graphene with specific twist angle,[34] and moiré excitons emerged in TMDs heterostructures.[35–38] More intriguing phenomenon has also been discovered in twisted bilayer heterojunction, including bandgap opening in graphene with adhering hexagonal boron nitride (h-BN),[39–41] and strong electron–phonon interaction at TMDs/h-BN interface.[42] Previously, the SHG from TMDs bilayer/heterostructures has been explored, which can be descried by the vector superposition of the SHG electric fields from the individual components.[43] However, direct modulation of nonlinear optical properties of one layer by another with van der Waals interaction remains largely unexplored.

In this article, we demonstrate that the nonlinear optical responses of 2D materials can be efficiently modulated by exciton oscillator strength under resonant excitation through the modification of the local dielectric environment. Moreover, with restraining the excitons formation by electron doping, this SHG modulation behavior will become faint, exhibiting appealing flexibility in the real device application designing.

2. Methods

Synthesis of MoS_2 MoS_2 monolayer samples were grown on SiO_2 substrate with 300 nm. 10 mg of MoO_3 (99%, Sigma-Aldrich) powder and 2 mg of NaCl (Greagent, 99.95%) were mixed and placed at the center of a tube furnace and 1 g of sulfur (99%, Sigma-Aldrich) powder was placed upstream of a quartz tube. The SiO_2 substrate was placed downstream 8 cm away from the Mo source. The chamber of the furnace was then flushed with argon for an inert atmosphere and subsequently ramped up to the optimized growth temperature (∼780 ℃) with 100 sccm argon. During growth process, the temperature for sulfur evaporation was ∼ 115 ℃. The entire process was carried out under ∼150 Pa and the growth duration was set as 10 min. After the growth, the system was naturally cooled to room temperature.

Heterostructure preparation MoS_2 was grown on SiO_2 substrate by chemical vapor deposition method. The graphene monolayer, graphene few-layer, and h-BN were mechanically exfoliated directly on PDMS films. Then, we stamped the PDMS films on the Si/SiO_2 substrate with MoS_2 and slowly released the PDMS. Contacts to the monolayer graphene flake were made using electron-beam evaporation.

PL and Raman measurements All the PL and Raman data were measured by self-built experimental equipment with 532 nm CW solid-state laser. The integral time was set as 5 s for PL measurements and laser power was set as 1 mW. The integral time was 60 s for the Raman measurements under the excitation of 2 mW laser power.

SHG measurements Wavelength-dependent SHG spectra were measured by using Coherent Vitara-T oscillator and optical parametric amplifier (OPA) 9850 laser system (∼70 fs, 250 kHz, 1200–1600 nm) excitation. Excitation laser was focused by a Nikon objective (60×, $NA = 0.65$) and the SHG signal was collected by the same Nikon objective with reflection mode. Through filtering out the excitation laser with a 700 nm short pass filter, SHG signal was recorded by the Princeton SP2500 spectrometer equipped with a nitrogen cooled Si charge coupled devices (CCD). All the experiments were done at room temperature.

3. Results and discussion

In this work, mechanical exfoliated graphene monolayer was transferred onto chemical vapor deposition (CVD) grown MoS_2 monolayer on 300 nm SiO_2/Si substrate via dry transfer method (Fig. 1(b)). The samples were firstly characterized via Raman and photoluminescence (PL) spectra (Fig. S1). In the Raman spectrum of individual MoS_2 and graphene, the standard characteristic peak position and intensity indicate their high quality and monolayer nature. The Raman intensity of MoS_2 is enhanced by ∼1.5 times in the heterostructure, indicating a clean and strongly coupled interface.[44] This interfacial coupling effect can also be observed in the PL spectra, where the PL intensity in MoS_2/graphene heterostructure is quenched to 10% because of electronic coupling and the associated charge/energy transfer process.[44]

The nonlinear optical response of monolayer MoS_2 was investigated in the atmosphere at room temperature. Under excitation with fundamental frequency ω, the strong second-order susceptibility $\chi^{2\omega}$ of MoS_2 leads to nonlinear polarization $P^{2\omega} = \varepsilon_0 \chi^{2\omega} E^{\omega} E^{\omega}$ and distinct SHG response. As expected, under femtosecond excitation at 1300 nm, a reflected SHG signal with peak centered at 650 nm was collected (Fig. 1(c)). This frequency harmonic generation phenomenon arises from the up-conversion process which requires instantaneous capture of two near-infrared photons to generate a visible photon. Therefore, the radiated SHG intensity obeys a squared dependence on the fundamental excitation power as shown in Fig. 1(d), where a double-logarithm representation is used for clarity.

Figures 2(a) and 2(b) show the SHG spectra of MoS_2 and MoS_2/graphene heterostructure, where totally different behaviors are exhibited under different wavelength excitation. For 1326 nm excitation, the SHG peak intensity of MoS_2/graphene weakened to 45% compared with that of pristine MoS_2 (Fig. 2(a)). However, the SHG peak intensity enhanced to 130% in the MoS_2/graphene heterostructure with excitation wavelengths of 1420 nm (Fig. 2(b)). As graphene monolayer is inversion symmetric, the second-order optical nonlinearity is electric-dipole forbidden and no SHG signal can be generated. Therefore, the variation of SHG must stem from the modulation of MoS_2 by graphene covering.

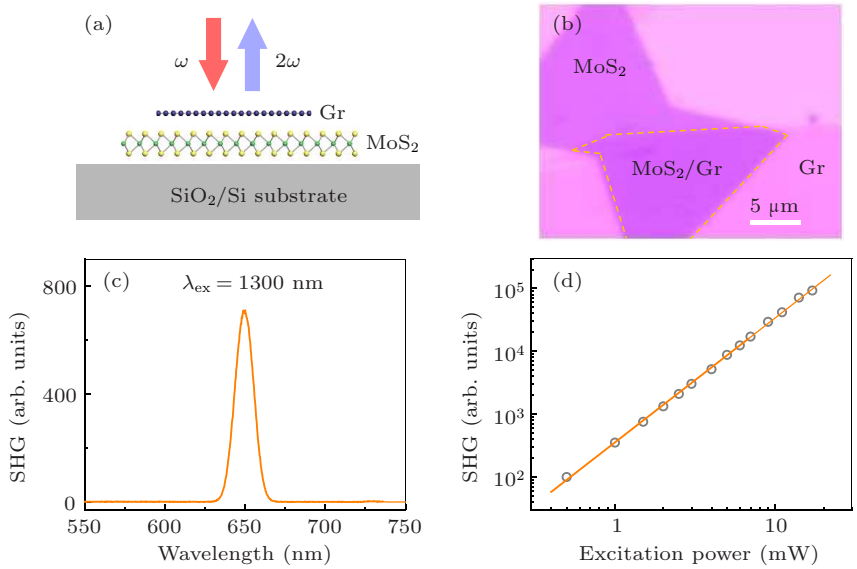


Fig. 1. SHG in MoS_2/graphene heterostructure. (a) Schematic illustration of optical SHG experiments on MoS_2 monolayer and MoS_2/graphene heterostructure. (b) Optical image of MoS_2/graphene. Exfoliated monolayer graphene was transferred on the top of CVD grown monolayer MoS_2 forming MoS_2/graphene heterostructure (in dashed line). Scale bar is 5 μm. (c) Optical SHG spectrum of MoS_2 monolayer under excitation of 1300 nm. (d) The power dependence of SHG peak intensity shows the expected quadratic dependence.

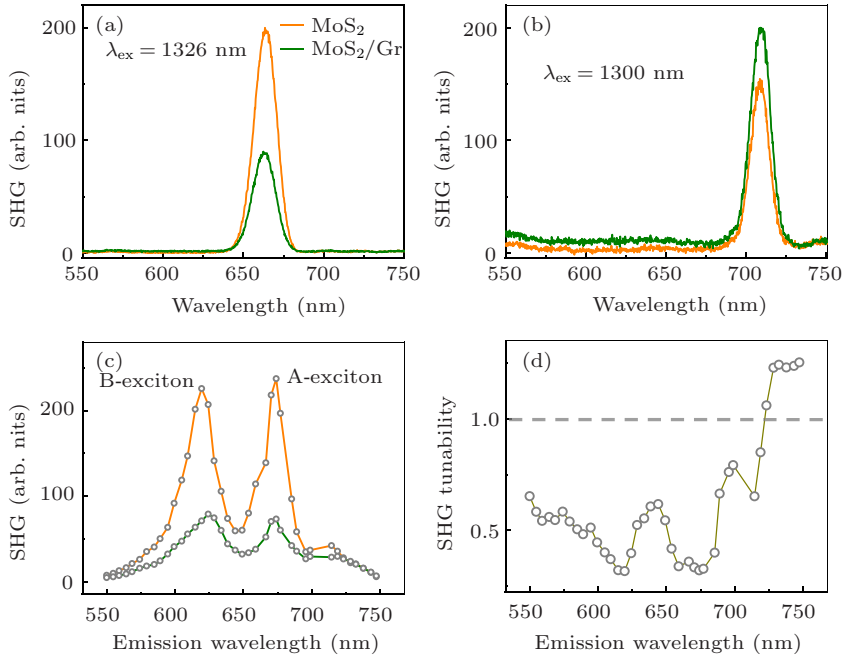


Fig. 2. Wavelengthdependent SHG modulation in MoS_2/graphene heterostructure. (a) Optical SHG spectra of monolayer MoS_2 and MoS_2/graphene heterostructure under excitation of 1326 nm, where the SHG decreased to 45% in the heterostructure. (b) SHG spectra of MoS_2 monolayer and MoS_2/graphene heterostructure under excitation of 1420 nm, where the SHG enhanced up to 130% in the heterostructure. (c) Wavelength-dependent SHG intensity of monolayer MoS_2 and MoS_2/graphene heterostructure. Both curves show peaks around MoS_2 A-exciton and MoS_2 B-exciton. (d) The SHG tenability, which describes the SHG intensity of MoS_2/graphene to that of MoS_2, is plotted. With interfacing graphene, the SHG intensity attenuated to ∼30% under resonance excitation, while slightly enhanced under off-resonance excitation.

To further understand this SHG engineering performance, we measured the excitation wavelength dependent SHG spectra of MoS_2/graphene heterostructure and MoS_2 monolayer with tuning excitation wavelengths (Fig. 2(c)). All the two wavelength dependent curves feature two prominent peaks at 675 nm and 620 nm, corresponding to A-exciton and B-exciton of MoS_2, respectively.[1] Under resonance excitation of exciton states, the SHG intensity is significantly enhanced due to the enhanced light–matter interaction and exciton dipole with strong oscillator strength.[13] The SHG tunability, which is defined as the ratio of the SHG intensity in MoS_2/graphene to that in pristine MoS_2, is plotted in Fig. 2(d). Wavelength dependent SHG tunability shows that the on-resonance excitation of exciton brings SHG intensity abatement while off-resonance excitation gives SHG intensity enhancement after graphene covering.

This on-resonance SHG weakening can also be gate tunable. Figure 3(a) shows the schematic diagram of our de-

vice, where ion-gel gating was used to controllably tune the chemical potential of the sample. By applying positive gate voltage V_g, the heterostructure will be electron doped, while negative gate voltage means hole doped. As our CVD grown MoS_2 samples are electron doped in nature, the application of a negative gate voltage will bring MoS_2 to charge neutral (Fig. S2). As expected, SHG spectra of both monolayer MoS_2 and MoS_2/graphene heterostructure show significant gate tunability under on-resonance excitation of 1340 nm (Fig. S3). Their SHG intensity reaches the maximum at $V_g = -1$ V, and show continuous decrease with voltage increase (Fig. 3(b)). Figure 3(c) shows the gate-dependent SHG tunability of MoS_2 with graphene covering. The SHG tunability is about 43% when V_g is between -2 V and 0 V, where MoS_2 is charge-neutral and A-exciton dominates the optical properties. When V_g goes positive and the formation of charge-neutral exciton is suppressed, on-resonance SHG weakening becomes faint.

We first discuss the on-resonance SHG weakening after covering graphene monolayer. There are mainly three scenarios that could be responsible for this SHG weakening: energy/charge transfer, charge doping, and dielectric screening effect. Though charge/energy transfer process is a common cause for PL quenching, it seems not possible for nonlinear optical signal decrease observed here. The parametric SHG process, which occurs instantaneously during the excitation pulse (~100 fs in our experiments), is ahead the charge/energy transfer process which takes scores of picoseconds after photoexcitation.[44–46] Meanwhile, the charge/energy transfer process is generally excitation wavelength independent, which happens at both the band edge and deep band in MoS_2. This is in contrast with the wavelength-dependent SHG modulation we observed. Charge doping can also be excluded from the primary causes, as the SHG intensity of MoS_2 without gating ($V_g = 0$ V) is higher than that of MoS_2/graphene at any doping level (Fig. 3(b)).

Dielectric screening effect is believed to be the most reasonable mechanism that responds to the SHG weakening. With graphene covering, the interaction strength between electron and hole in an exciton decreases, resulting in a reduction in spatial overlapping in MoS_2. As a result, the exciton oscillator strength would be diminished according to the Fermi golden rule (Fig. 4(a)). Since the exciton effects mainly contribute to the SHG response under resonant excitation, the decrease of exciton oscillator strength with graphene covering will surely bring the wavelength-dependent SHG modulation where the SHG weakens under resonance excitation.

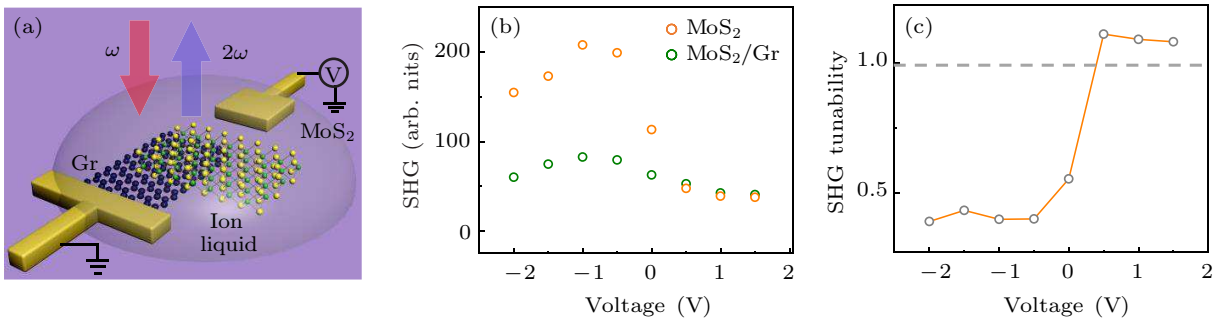


Fig. 3. Gate-dependent SHG in MoS_2 monolayer and MoS_2/graphene heterostructure. (a) Schematic of gated MoS_2/graphene via ion-gel. (b) Gate voltage dependent SHG in monolayer MoS_2 and MoS_2/graphene. As our CVD grown MoS_2 is electron doped in nature, the application of negative gate voltage will bring MoS_2 to charge neutral and decline SHG intensity for both MoS_2 monolayer and MoS_2/graphene heterostructure. (c) SHG tunability at different gate voltage. At negative gate voltage where MoS_2 is charge-neutral, the SHG tunability can reach 43%. When the gate voltage goes positive and the formation of charge-neutral exciton is suppressed, SHG modulation behavior will become faint. SHG of monolayer MoS_2 is nearly the same as that of heterostructure.

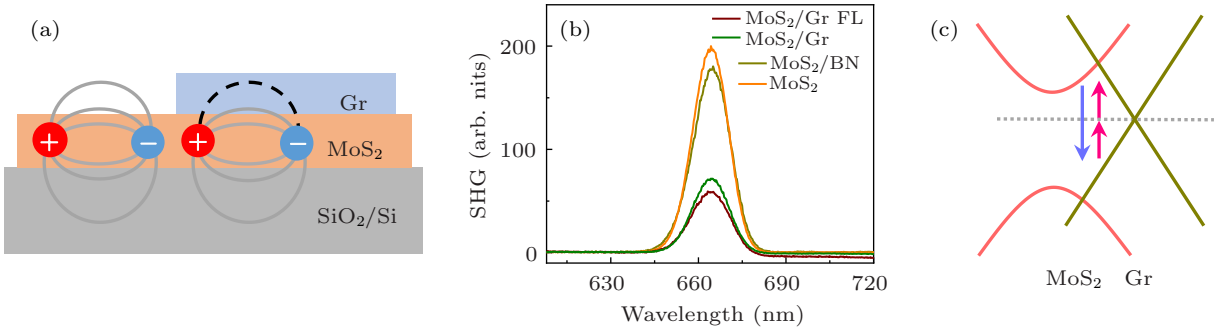


Fig. 4. Mechanisms of SHG modulation in MoS_2 by graphene covering. (a) Schematic illustration of dielectric screening effect in MoS_2/graphene heterostructure. With graphene covering, the interaction strength between electron and hole in an exciton decreases, resulting in oscillator strength diminishing. (b) Optical SHG spectra of MoS_2, MoS_2/BN, MoS_2/graphene, and MoS_2/Gr few-layer under excitation of 1330 nm. Serving as strong screening dielectric material, graphene declines the SHG intensity of MoS_2 monolayer to 35% at excitation resonance. For MoS_2/Gr few-layer, the SHG further reduces to 30%. While for the covering of insulating h-BN, MoS_2 SHG intensity only decreases to 90%. (c) Schematic of interlayer excitation SHG between MoS_2 and graphene, which may response for the SHG enhancement under off-resonance excitation.

In the following, we used different dielectric materials to test the screening strength and modulate the SHG intensity. As graphene is semimetal with abundant free carriers and hence provides a strong dielectric screening, the SHG of MoS_2 monolayer weakens to ~35% after adhering monolayer graphene. While for the covering of insulating BN, MoS_2 SHG intensity only decreases to 90% (Fig. 4(b)). Graphene few layers with stronger screening effect bring deeper SHG tunability to ~30%.

Afterwards, we elucidate the mechanism of SHG enhancement with graphene covering under off-resonant excitation. Hot carrier injection and interlayer transition are two main physical processes under near infrared laser excitation, where $2\hbar\omega$ is smaller than the bandgap of MoS_2. Under this condition, MoS_2 is silent with light while graphene can still be excited. The photoexcited hot electrons (rather than holes, because of the band alignment of graphene and MoS_2 shown in Fig. 4(c)) in graphene have chance to overcome the interlayer barrier and inject to MoS_2. While electron doping will decrease the SHG intensity, as we have discussed. Therefore, the hot carrier injection from graphene to MoS_2 cannot be the reason of SHG enhancement we observed. Interlayer excitation between MoS_2 and graphene is conjectured to be the most possible mechanism for the SHG enhancement after graphene covering (Fig. 4(c)). SHG from the heterostructure mainly contains two parts, i.e., one from interaction of virtual states in monolayer MoS_2, and the other from real states transition between the valence band of graphene and conduction band of MoS_2. Under on-resonant excitation, the former one dominates the SHG intensity and the later one can be neglect. As the excitation wavelength increases to off-resonance, the SHG intensity from the former one drops significantly and the later one becomes observable, resulting in the SHG enhancement we detected.

4. Conclusion

In summary, we developed a new method to modulate the SHG of MoS_2 by covering graphene. The SHG intensity of MoS_2/graphene heterostructure was proved to be suppressed at exciton-resonance regime while enhanced away from resonance, correspondingly attributed to the dielectric screening effect and interlayer excitation. Our work has taken a tentative step in dielectric tuning of SHG in 2D materials and promoted deeper understanding in the exciton behaviors. Moreover, our discovery of nonlinear optical response modulation through surrounding dielectric tuning will be very instructive in the design of future nonlinear optoelectrical devices based on 2D materials.

References

[1] Mak K F, Lee C, Hone J, Shan J and Heinz T F 2010 *Phys. Rev. Lett.* **105** 136805
[2] Mak K F, He K, Shan J and Heinz T F 2012 *Nat. Nanotechnol.* **7** 494
[3] Cao T, Wang G, Han W, Ye H, Zhu C, Shi J, Niu Q, Tan P, Wang E, Liu B and Feng J 2012 *Nat. Commun.* **3** 887
[4] Zeng H, Dai J, Yao W, Xiao D and Cui X 2012 *Nat. Nanotechnol.* **7** 490
[5] Jones A M, Yu H, Ghimire N J, Wu S, Aivazian G, Ross J S, Zhao B, Yan J, Mandrus D G, Xiao D, Yao W and Xu X 2013 *Nat. Nanotechnol.* **8** 634
[6] Ye Z, Cao T, O'Brien K, Zhu H, Yin X, Wang Y, Louie S G and Zhang X 2014 *Nature* **513** 214
[7] Fei Z, Palomaki T, Wu S, Zhao W, Cai X, Sun B, Nguyen P, Finney J, Xu X and Cobden D H 2017 *Nat. Phys.* **13** 677
[8] Liu X J and Zhang Y W 2018 *Chin. Phys. B* **27** 034402
[9] Wang J, Guo C, Guo W L, Wang L, Shi W Z and Chen X S 2019 *Chin. Phys. B* **28** 046802
[10] Hung T Y T, Rustagi A, Zhang S J, Upadhyaya P and Chen Z H 2020 *Infomat* **2** 968
[11] Zou C J, Zhang H B, Chen Y, Feng S, Wu L S, Zhang J, Yu T, Shang J Z and Cong C X 2020 *Infomat* **2** 585
[12] Li Y, Rao Y, Mak K F, You Y, Wang S, Dean C R and Heinz T F 2013 *Nano Lett.* **13** 3329
[13] Wang G, Marie X, Gerber I, Amand T, Lagarde D, Bouet L, Vidal M, Balocchi A and Urbaszek B 2015 *Phys. Rev. Lett.* **114** 097403
[14] Liu H, Li Y, You Y S, Ghimire S, Heinz T F and Reis D A 2016 *Nat. Phys.* **13** 262
[15] Saynatjoki A, Karvonen L, Rostami H, Autere A, Mehravar S, Lombardo A, Norwood R A, Hasan T, Peyghambarian N, Lipsanen H, Kieu K, Ferrari A C, Polini M and Sun Z 2017 *Nat. Commun.* **8** 893
[16] Wen X L, Gong Z B and Li D H 2019 *Infomat* **1** 317
[17] Zeng Z X S, Wang X and Pan A L 2020 *Acta Phys. Sin.* **69** 184210 (in Chinese)
[18] Yin X B, Ye Z L, Chenet D A, Ye Y, O'Brien K, Hone J C and Zhang X 2014 *Science* **344** 488
[19] Cheng J, Jiang T, Ji Q, Zhang Y, Li Z, Shan Y, Zhang Y, Gong X, Liu W and Wu S 2015 *Adv. Mater.* **27** 4069
[20] Guo J, Zhao J L, Huang D Z, Wang Y Z, Zhang F, Ge Y Q, Song Y F, Xing C Y, Fan D Y and Zhang H 2019 *Nanoscale* **11** 6235
[21] Cheng Y, Hong H, Zhao H, Wu C, Pan Y, Liu C, Zuo Y, Zhang Z, Xie J, Wang J, Yu D, Ye Y, Meng S and Liu K 2020 *Nano Lett.* **20** 8053
[22] Lee J, Tymchenko M, Argyropoulos C, Chen P Y, Lu F, Demmerle F, Boehm G, Amann M C, Alu A and Belkin M A 2014 *Nature* **511** 65
[23] Cheng J L, Vermeulen N and Sipe J E 2014 *New J. Phys.* **16** 053041
[24] Aouani H, Rahmani M, Navarro-Cia M and Maier S A 2014 *Nat. Nanotechnol.* **9** 290
[25] Seyler K L, Schaibley J R, Gong P, Rivera P, Jones A M, Wu S F, Yan J Q, Mandrus D G, Yao W and Xu X D 2015 *Nat. Nanotechnol.* **10** 407
[26] Liang J, Zhang J, Li Z Z, Hong H, Wang J H, Zhang Z H, Zhou X, Qiao R X, Xu J Y, Gao P, Liu Z R, Liu Z F, Sun Z P, Meng S, Liu K H and Yu D P 2017 *Nano Lett.* **17** 7539
[27] Jiang T, Huang D, Cheng J L, Fan X D, Zhang Z H, Shan Y W, Yi Y F, Dai Y Y, Shi L, Liu K H, Zeng C G, Zi J, Sipe J E, Shen Y R, Liu W T and Wu S W 2018 *Nat. Photon.* **12** 634
[28] Soavi G, Wang G, Rostami H, Purdie D G, De Fazio D, Ma T, Luo B R, Wang J J, Ott A K, Yoon D, Bourelle S A, Muench J E, Goykhman I, Dal Conte S, Celebrano M, Tomadin A, Polini M, Cerullo G and Ferrari A C 2018 *Nat. Nanotechnol.* **13** 583
[29] Wen X L, Xu W G, Zhao W J, Khurgin J B and Xiong Q H 2018 *Nano Lett.* **18** 1686
[30] Shi J J, Li Y, Kang M, He X B, Halas N J, Nordlander P, Zhang S P and Xu H X 2019 *Nano Lett.* **19** 3838
[31] Hong H, Liu C, Cao T, Jin C, Wang S, Wang F and Liu K 2017 *Adv. Mater. Interfaces* **4** 1601054
[32] Wang G C, Wu L M, Yan J H, Zhou Z, Ma R S, Yang H F, Li J J, Gu C Z, Bao L H, Du S X and Gao H J 2018 *Chin. Phys. B* **27** 077303
[33] Cheng Y, Huang C, Hong H, Zhao Z X and Liu K H 2019 *Chin. Phys. B* **28** 107304
[34] Cao Y, Fatemi V, Fang S, Watanabe K, Taniguchi T, Kaxiras E and Jarillo-Herrero P 2018 *Nature* **556** 43
[35] Alexeev E M, Ruiz-Tijerina D A, Danovich M, Hamer M J, Terry D J, Nayak P K, Ahn S, Pak S, Lee J, Sohn J I, Molas M R, Koperski M, Watanabe K, Taniguchi T, Novoselov K S, Gorbachev R V, Shin H S, Fal'ko V I and Tartakovskii A I 2019 *Nature* **567** 81

[36] Jin C, Regan E C, Yan A, Iqbal Bakti Utama M, Wang D, Zhao S, Qin Y, Yang S, Zheng Z, Shi S, Watanabe K, Taniguchi T, Tongay S, Zettl A and Wang F 2019 *Nature* **567** 76

[37] Seyler K L, Rivera P, Yu H, Wilson N P, Ray E L, Mandrus D G, Yan J, Yao W and Xu X 2019 *Nature* **567** 66

[38] Tran K, Moody G, Wu F, *et al*. 2019 *Nature* **567** 71

[39] Hunt B, Sanchez-Yamagishi J D, Young A F, Yankowitz M, LeRoy B J, Watanabe K, Taniguchi T, Moon P, Koshino M, Jarillo-Herrero P and Ashoori R C 2013 *Science* **340** 1427

[40] Ponomarenko L A, Gorbachev R V, Yu G L, Elias D C, Jalil R, Patel A A, Mishchenko A, Mayorov A S, Woods C R, Wallbank J R, Mucha-Kruczynski M, Piot B A, Potemski M, Grigorieva I V, Novoselov K S, Guinea F, Fal'ko V I and Geim A K 2013 *Nature* **497** 594

[41] Dean C R, Wang L, Maher P, Forsythe C, Ghahari F, Gao Y, Katoch J, Ishigami M, Moon P, Koshino M, Taniguchi T, Watanabe K, Shepard K L, Hone J and Kim P 2013 *Nature* **497** 598

[42] Jin C H, Kim J, Suh J, Shi Z W, Chen B, Fan X, Kam M, Watanabe K, Taniguchi T, Tongay S, Zettl A, Wu J Q and Wang F 2017 *Nat. Phys.* **13** 127

[43] Hsu W T, Zhao Z A, Li L J, Chen C H, Chiu M H, Chang P S, Chou Y C and Chang W H 2014 *Acs Nano* **8** 2951

[44] He J Q, Kumar N, Bellus M Z, Chiu H Y, He D W, Wang Y S and Zhao H 2014 *Nat. Commun.* **5** 5622

[45] Yuan L, Chung T F, Kuc A, Wan Y, Xu Y, Chen Y P, Heine T and Huang L B 2018 *Sci. Adv.* **4** e1700324

[46] Chen Y Z, Li Y J, Zhao Y D, Zhou H Z and Zhu H M 2019 *Sci. Adv.* **5** eaax9958